Macromolecules

pubs.acs.org/Macromolecules Article

Three-Dimensional Covalent Organic Framework Membranes: Synthesis by Oligomer Interfacial Ripening and Application in Precise Separations

Xiansong Shi, Zhe Zhang, Mingjie Wei, Xingyuan Wang, Jingtao Wang, Yatao Zhang, and Yong Wang*

Cite This: *Macromolecules* 2022, 55, 3259−3266 Read Online

ACCESS | Metrics & More | Article Recommendations | Supporting Information

ABSTRACT: Covalent organic framework (COF) membranes are viable to tackle intractable separations, thanks to their uniform configurations and devisable functions. However, in stark contrast to the intensively studied two-dimensional COF membranes, three-dimensional (3D) COF membranes with unique merits remain largely unexplored because of formidable synthetic obstacles. Herein, we report a novel method to produce robust 3D COF membranes with interpenetrated nanochannels by ripening presynthesized oligomers at the organic−water interface. With the amphiphilicity and appropriate size, oligomers are prone to be entrapped at the designed interface. The ripening of interface-captured oligomers generates self-supporting crystalline 3D COF membranes with controllable thicknesses. The resulting membranes are provided with uniformly interpenetrated nanochannels, of which the aperture sizes ranging from ∼0.8 to 1.5 nm can be tailor-made by monomer design. We further identify the prominent competence of these 3D COF membranes in the high-precision fractionation of ions and molecules. Particularly, the sub-nanometer channels of the 3D COF-1 membrane allow for the efficient sieving of mono- and multivalent ions, attaining a K^+/Al^{3+} selectivity of >800. This work reports a facile but efficient strategy to synthesize COF membranes and opens up the applications of 3D COFs in the precise separation of ions and fine molecules.

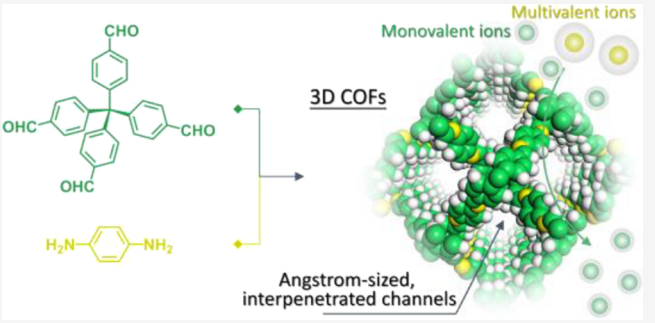

INTRODUCTION

Covalent organic frameworks (COFs) are an emerging class of perforated crystalline polymers with permanent porosities and high-order nanochannels, whose topological structures and physicochemical properties are predesignable.[1,2] The synthesis of COFs involves the coexistence of polymerization and crystallization, in which the polymer chain growth and structural ordering proceed concurrently. The growth of polymer chains refers to the polycondensation between COF monomers, which produces highly cross-linked frameworks having polymer characteristics. The major difference between polymer networks and COFs is the structural regularity, corresponding to the amorphous and crystalline nature, respectively. In spite of this, the conversion of amorphous polymers into crystalline COFs can be realized by the exchange of building blocks.[3] Moreover, the design and synthesis of COF materials still strongly rely on the polymer science.[4] To be specific, the monomer geometry primarily determines the chain growth behavior of polymers, which affords the guidance for the topologic design of COFs through the geometric combination of monomers. As an emerging class of polymers, the functionalization of COFs is also directed by polymer science, following the presynthetic and postsynthetic methodologies. Thus, by taking advantage of the knowledge and practices in the aspect of polymer design, polymerization, functionalization, and characterizations accumulated in the field of polymer science in the past half century, COFs have made great progress and show tremendous potential in various fields including electrochemistry, catalysis, energy and gas storage, and separation.[5] Since the first report of COFs by Yaghi and co-workers in 2005,[6] a wealth of COFs with rationally designed linkages and topologies have been synthesized, giving rise to an enriched structural diversity and expanded applications. According to the spatial connectivity of covalent bands, COFs can be classified as two-dimensional (2D) and three-dimensional (3D) types, which are constructed by planar and tri-dimensional building units, respectively. Typically, 2D COFs present layered structures with perpendicular channels, while 3D COFs feature interpenetrated and cage-like channels.[7] The structural design of 3D COFs mainly focuses on the exploration of new topologies

Received: November 11, 2021
Revised: March 23, 2022
Published: April 8, 2022

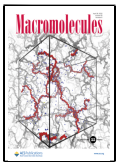

https://doi.org/10.1021/acs.macromol.1c02333
Macromolecules 2022, 55, 3259−3266

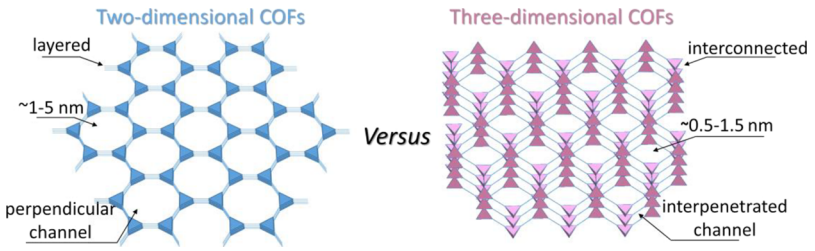

Figure 1. Comparison between layered eclipsed 2D and diamond-like 3D COFs.

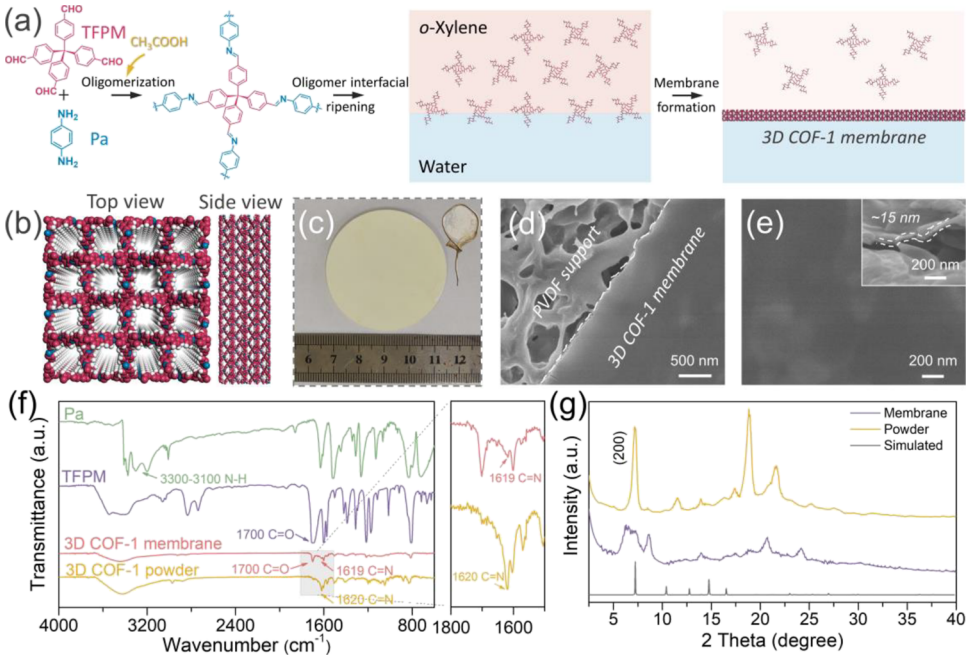

Figure 2. Synthesis of 3D COF-1 membranes by oligomer interfacial ripening. (a) Illustration of the synthesis procedure; (b) structure of 3D COF-1; photograph (c) and surface SEM images (d,e) of the 3D COF-1 membrane with a synthesis duration of 1 h transferred on a macroporous PVDF substrate; (f) FTIR spectra; and (g) PXRD patterns. Inset in (e) is the cross-sectional SEM image of the 3D COF-1 membrane.

and building blocks. Inspired by the progress on 2D COFs, the research interest of 3D COFs is continuously growing in recent years.

Compared to the vast reports on the syntheses and applications of 2D COFs, research efforts on 3D COFs are sparse mostly because of the shortage of available monomers as well as challenges in synthesis and structural identification.[7] Especially, for size-discriminating separations, which strongly depend on the pore uniformity,[8] 2D COFs have been recognized as prospective materials for producing advanced membranes.[9] So far, dozens of 2D COF-based membranes have been successfully synthesized by different methods, yielding excellent performances in separation-related fields.[10] However, existing 2D COF membranes often have relatively large pore sizes in the range of 1−5 nm (Figure 1), which allows them to be merely applicable for separating large targets like dyes and nanoparticles.[11−13] As a consequence, 2D COF membranes are inevitably inferior in tackling the gaseous and ionic targets.[14] To cope with this limitation, complicated and tedious modification procedures are usually required, for example, shrinking the effective sieving sizes by postsynthetic modification, or introducing charge exclusion by pore engineering.[15−17] Moreover, isolated 1D channels with no interconnectivity are involved in 2D COF membranes, potentially limiting the mass transfer efficiency.

3D COFs are provided with three-dimensionally interconnected pathways and possess more void spaces that contribute a higher porosity (Figure 1), ideally suitable for mass transport.[7,18] The interlaced skeletons of 3D COFs narrow down the aperture sizes into the range of ~0.5−1.5 nm,[7] which promise the ultimate separation of ions and gases. By virtue of the pore-connected backbone, 3D COFs have more open sites that are accessible for accurate functionalization, thus offering the membrane designability for specific separation applications. For example, Jiang and co-workers have demonstrated the superiority of 3D COF membranes for efficient proton conduction.[19] In our very recent study, the polyimide-supported 3D COF membranes exhibited great potential for robust molecular separations.[20] Therefore, the benefits in structures and functions make 3D COFs ideal candidates for constructing membranes for ion separation. Excitingly, this has been confirmed by simulation works.[21] Unfortunately, the experimental exploration of 3D COFs in ion separations still lacks profound studies. It is undoubted that additional criteria, such as water resistance and mechanical stability, should be seriously considered when applying 3D COFs in liquid separations. Nevertheless, only a few chemical reactions and Schiff base reactions, for example, are so far developed to produce 3D COFs with sufficient stability in water.[10] A membrane synthetic strategy is another obstacle that impedes

https://doi.org/10.1021/acs.macromol.1c02333
Macromolecules 2022, 55, 3259−3266

the use of 3D COFs in this field. Numerous strategies including solvothermal synthesis, interfacial crystallization, and the assembly of COF nanosheets have been developed to prepare 2D COF membranes,[9] but producing 3D COF membranes through a facile and effective strategy remains a synthetic challenge. Heretofore, due to the absence of a facile strategy, harsh synthetic conditions are usually requisite to ensure the integrity of 3D COF membranes.[22,23]

Herein, we propose a general and facile approach to synthesize imine-linked 3D COF membranes by ripening preformed oligomers at the organic−water interface under room temperature. Based on this strategy, a series of 3D COF membranes are synthesized with elaborately designed aperture sizes by reacting a tetrahedral aldehyde with size-varied amine linkers. Interestingly, the obtained 3D COF membranes with a thickness of ∼15 nm exhibit excellent robustness and moderate crystallinity. Owning to the uniform, interconnected microporous channels, the membranes display sharp selectivities in discriminating monovalent ions over multivalent ions and in the sieving of targeted small molecules from their similarly sized mixtures.

RESULTS AND DISCUSSION

Figure 2a represents the oligomer structure and preparation of 3D COF-1 membranes through the oligomer interfacial ripening at the organic−water interface. The formation of 3D COF membranes is distinctive from previously reported studies involving an in situ nucleation or crystallization from molecular monomers.[24−26] Here, the preparation process can be mainly divided into two steps, oligomerization of monomers and interfacial ripening of oligomers. By introducing acetic acid as the catalyst, we first triggered the mild condensation between the two monomers, producing oligomers which form highly stable dispersions in *o*-xylene (Figure S5). Notably, the mixture produced by simply mixing the monomer solutions was clear and transparent, but immediately became yellowish upon the addition of acetic acid (Figure S6a). The color change implies the formation of oligomers, which is confirmed by an intense Tyndall effect (Figure S6b). The oligomerization induced by acetic acid was analyzed by an UV−vis spectrophotometer. The mixture without acetic acid only displays the characteristic peaks of monomers, while new peaks emerge upon the addition of acetic acid (Figure S7). The matrix-assisted laser desorption ionization time-of-flight mass spectrometry also confirms the oligomerization between monomer pairs (Figure S8). The 3D COF-1 membrane was then synthesized by spreading the oligomer dispersion onto the surface of water followed by ripening at the interface. In the membrane formation, the interfacial entrapment of oligomers is crucial for the ripening to generate continuous membranes, which mainly depends on the size and amphiphilicity of oligomers.[27] It can be seen from Figure S9 that the smallest oligomers have a lateral size of ∼2.4 nm. The size obviously exceeds the smallest particle size (∼1.6 nm) required for the stable residence at organic−aqueous interfaces.[28] We also checked the water contact angle of the synthesized 3D COF-1 membrane, and they present a contact angle of ∼78° (Figure S10a), stating a relatively neutral affinity of 3D COF-1 to both *o*-xylene and water. Accordingly, when the 3D COF-1 oligomers diffuse to the interface, they prefer to stably reside there without escaping due to their surface wettability being similar to water and *o*-xylene, as illustrated in Figure S10b.[29] After the entrapment of these oligomers at the interface, the catalysis of acetic acid facilitates the ripening of oligomers to form a continuous membrane. In the light of the reversibility of Schiff base reaction between amines and aldehydes, self-correction of defective areas happens during the growth of 3D COF-1 membranes, thus giving an ordered, crystalline extended framework (Figure 2b).[2] We can clearly observe a membrane confined at the organic−water interface within 1 h. The resulting membrane with a diameter >4 cm is free of any breakages (Figure 2c), which can be enlarged by using synthesis vessels with bigger interface areas (Figure S11). Surprisingly, the integrity of the membrane is well maintained after being repeatedly squeezed through a dropper (Movie S1), indicative of its robustness. Moreover, the membrane is strong enough to self-support as it can be easily transferred to and covered on a lasso (inset in Figure 2c). After transferring and compositing with a macroporous poly (vinylidene fluoride) (PVDF) substrate, the 3D COF-1 membrane presents a smooth surface without any pinholes, cracks, or other defects (Figure 2d). The scanning electron microscopy (SEM) image in Figure 1e reveals a low thickness of ∼15 nm for the produced 3D-COF-1 membrane. In contrast, the traditional interfacial crystallization by polymerizing molecular monomers at the interface leads to weak 3D COF-1 membranes that exhibit poor mechanical strength (Figure S12).

Fourier transform infrared (FTIR) spectroscopy was employed to survey the detailed structure of the resultant membranes and solvothermally synthesized powders. As shown in Figure 2f, the spectra display C═N stretching vibrations around 1619 cm^{-1} for 3D COF-1 membranes and 1620 cm^{-1} for 3D COF-1 powders, illustrating the occurrence of condensation to form imine-linked frameworks.[30] Together with the absence of amine N−H and aldehyde C═O stretching bands at 3300−3100 cm^{-1} and 1700 cm^{-1}, respectively, the sufficient consumption of starting monomers in the 3D COF powder is confirmed. The emergence and disappearance of the aforesaid peaks in the membrane are in good agreement with the results reported in literature.[30] The high-order structures of 3D COF-1 membranes and powders were ascertained by powder X-ray diffraction (PXRD) characterizations (Figure 2g). The peak at ∼7.2° for the powder and membrane corresponds to the (200) crystal facet, which is consistent with the simulation result and previous studies,[30] implying an interpenetrated diamond-like network. The peak at ∼8.65° in the membrane PXRD pattern may arise from a collapse of the (200) plane, resulting in a slightly reduced aperture size.[31] Taking the mild synthesis conditions into consideration, it is reasonable for the membrane to show moderate crystallinity. In addition, the low thickness and random stacking of membranes in PXRD tests could potentially compromise the peak intensity as well.[32] N_2 adsorption−desorption measurements were conducted at 77 K to analyze the porous structure of 3D COF-1. Figure S13a depicts that the 3D COF-1 powder has a sharp gas uptake at a relatively low pressure, indicating a prominent microporous porosity. Its Brunauer−Emmett−Teller (BET) surface area is as high as ∼486 $m^2\ g^{-1}$. By fitting nonlocal density functional theory, we identify a sub-nanometer pore size of ∼8.3 Å (Figure S13b). As a comparison, the 3D COF-1 synthesized by direct interfacial polymerization exhibits a low BET surface area < 10 $m^2\ g^{-1}$ (Figure S14). In addition, Young's modulus of the oligomerization-enabled 3D COF-1 membrane largely exceeds that of the membrane produced by direct interfacial polymerization (Figure S15). These complementary results

https://doi.org/10.1021/acs.macromol.1c02333
Macromolecules 2022, 55, 3259−3266

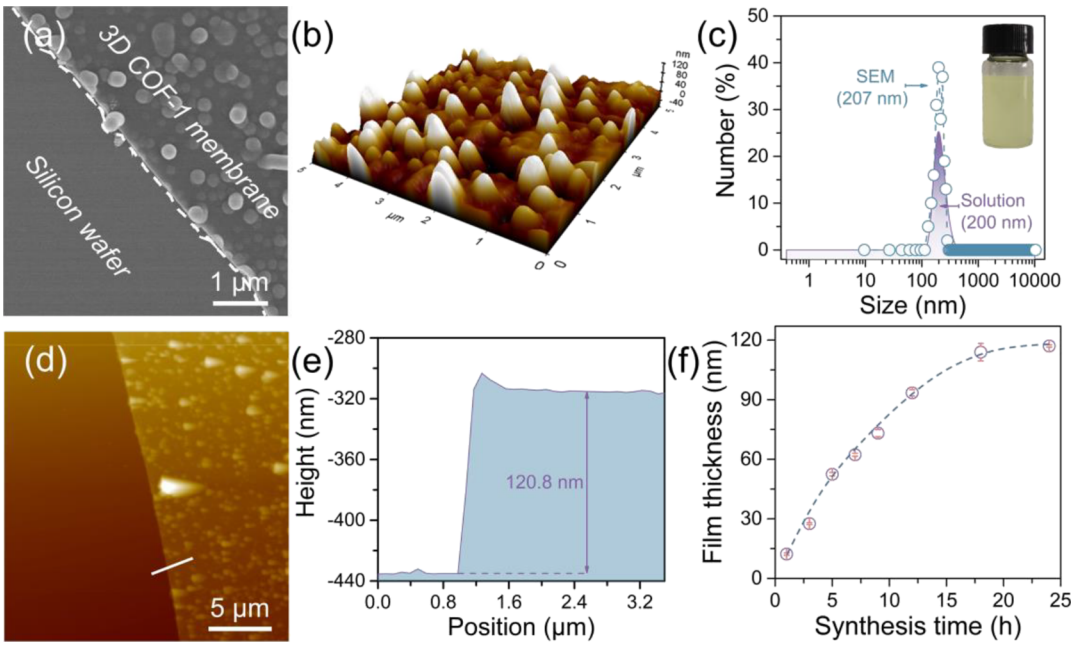

Figure 3. Structural characterizations of 3D COF-1 membranes transferred on silicon wafers. SEM (a) and AFM (b) images of the membrane after synthesizing for 12 h; (c) size distributions of COF spheres obtained from the DLS and SEM image; AFM image (d) of the membrane after synthesizing for 24 h and the corresponding height profile (e); (f) thicknesses of the membranes synthesized with various durations. Inset in (c) is the photograph of the synthesis solution with a 12 h reaction duration.

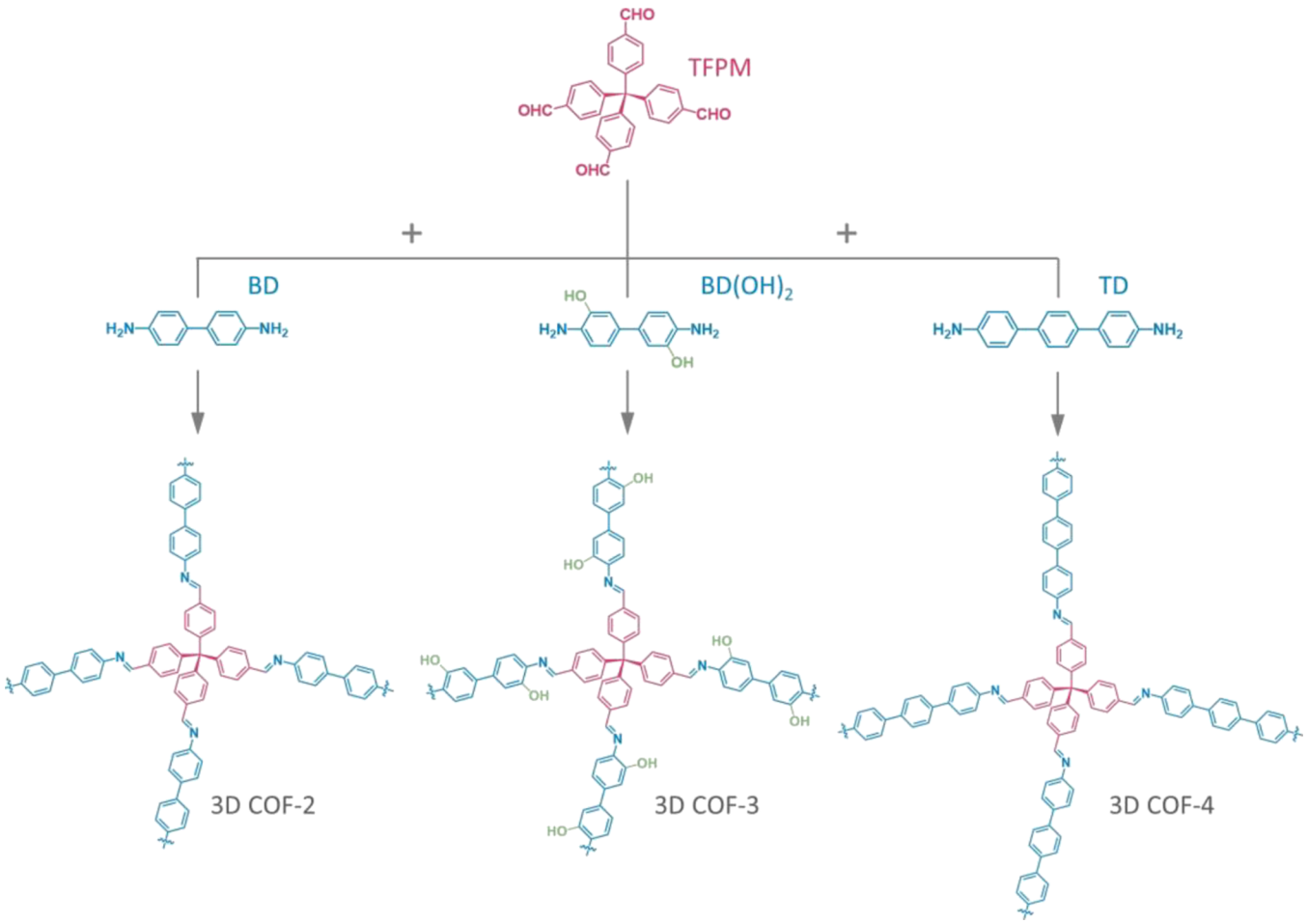

Figure 4. Synthesis of other 3D COF membranes by oligomer interfacial ripening.

https://doi.org/10.1021/acs.macromol.1c02333
Macromolecules 2022, 55, 3259−3266

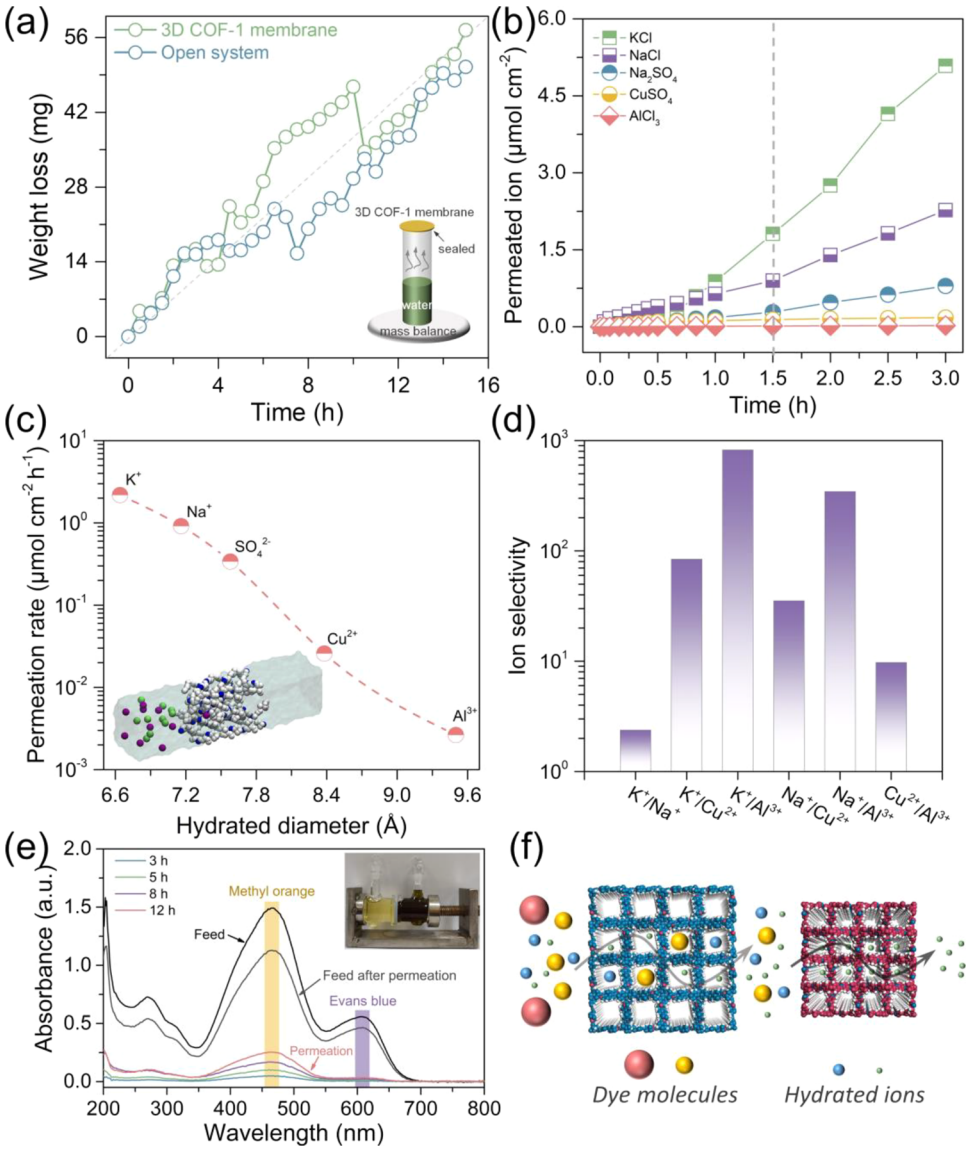

Figure 5. Separation performances of 3D COF membranes. (a) Water evaporation through the 3D COF-1 membrane; (b) ion diffusion of various inorganic salts; (c) diffusion rate of various ions; (d) ion selectivity of different ion pairs; (e) UV−vis spectra for the diffusion of dyes in the 3D COF-4 membrane; and (f) schematic diagram of 3D COF membranes with varied pore sizes toward molecular and ionic sieving. Inset in (e) is the photograph of the dye diffusion after 12 h.

confirm the validity of our oligomer interfacial ripening method.

The structural features of 3D COF-1 membranes were then systematically investigated by observing the morphology of membranes synthesized under diverse durations (Figure S16). Interestingly, the surface of these membranes changes from the smooth morphology to a massif-like one with the synthesis duration extended from 1 to 12 h (Figures 3a,b, and S17 and S18). Similar rugged structures are frequently observed from imine-linked COF membranes prepared by solvothermal growth;[14,33] however, the formation mechanism is unexposed. We speculate that the oligomers account for the formation of initial smooth membranes given their small sizes. Prolonging the ripening duration facilitates the polymerization of oligomers in the bulk organic solution to generate COF spheres, evidenced by the dynamic laser scattering (DLS) (Figure 3c). The COF spheres will inevitably deposit onto the surface of the smooth membranes due to gravity. Subsequently, the breaking and re-bonding of imine bonds based on the reversible reaction induce a coalescence of the smooth membranes and COF spheres, which integrates these two objects together to present a massif-like topography. The consistency of the size distribution obtained from the DLS and SEM images manifestly validates this coalescing process (Figure 3c), which is considered to be triggered by the mechanism of Ostwald ripening.[34] Because the crystallites in the COF sphere deliver much higher curvature, they possess higher surface energy compared with those in the sheet-like membrane. Therefore, upon contact, the outer crystallites of COF spheres tend to de-assemble and re-assemble with the terminal groups (i.e., amine and aldehyde) of membranes to minimize the surface energy, and this is the time that the integration occurs. In our work, adjusting the ripening duration may offer the viability of managing the membrane thickness. According to the atomic force microscopy (AFM) characterization, the membrane synthesized with a duration of 24 h has

https://doi.org/10.1021/acs.macromol.1c02333
Macromolecules 2022, 55, 3259−3266

a thickness of ∼120.8 nm (Figure 3d,e). The membrane thickness versus the synthesis duration was then studied by spectroscopic ellipsometry (Figure 3f). It is noteworthy that the thickness value obtained by ellipsometry coincides with the AFM result. The membrane thickness is highly tunable in the range of ∼12−120 nm by prolonging the duration from 1 to 24 h. The thickness increase in turn leads to the color change from buff to blue (Figure S19). Notably, the thickness growth rate gradually decreases with the synthesis duration, finally achieving a relatively constant thickness after 24 h. This can be attributed to the self-limiting nature of the interface-enabled synthesis.[35] After removing the initially formed membranes from the interface, reactions between unconsumed oligomers could resume, forming new membranes with similar morphologies (Figures S20 and S21).

To demonstrate the universality of the proposed synthesis strategy, we thereby prepared a series of 3D COF membranes by interfacially ripening presynthesized COF oligomers at the organic−water interface (Figure 4). The resultant membranes that have a large size of ∼3 × 3 cm^2 are visually transparent (Figure S22), stating their low thicknesses. These membranes display surface morphologies analogous to that of 3D COF-1 membranes, showing a relatively smooth surface with scattered particles. The structural feature supports the membrane formation mechanism stated before. A synthesis duration of 12 h produces membranes with a similar thickness of ∼100 nm for these 3D COFs (Figure S23). Thus, the interfacial ripening of oligomers is generally applicable to synthesize imine-linked 3D COF membranes, whose structures can be molecularly tailored by monomer design.

Encouraged by the prominent porosity and regular sub-nanometer channels of 3D COF-1, we expect that the resultant membrane could work as a promising platform for precise ion sieving. No penetration of small-sized dyes validates the membrane integrity (Figures S24 and S25). To confirm the inherently high and accessible porosity of 3D COF-1 membranes, the permeation of water vapor across the membrane supported by a porous anodic aluminum oxide (AAO) substrate was assessed (Figure S26). Figure 5a shows that the evaporation rate of the membrane-sealed container is similar with the open container, which evidently manifests the prominent porosity that allows for unimpeded flow of vapor.[36] Also importantly, the synthesized membranes are highly stable in water for weeks without any breakages (Figure S27), suggesting their ability for use in aqueous milieu. To evaluate the ion sieving performance of the 3D COF-1 membrane, the ion diffusion measurements were then performed using a home-made cell, where the 0.1 M ionic solution and water served as the draw and feed solution, respectively. Figure S28 gives the conductivities of all the salt solutions with a concentration of 0.1 M, and the conductivities are in the range of 8.5−25 mS cm^{-1}. Obviously, the diffusion of Na_2SO_4 in 20 nm AAO membranes is extremely faster (∼100 times higher) than that of the 3D COF-1 membrane (Figure S29). The result indicates the feasibility of sub-nanometer channels to regulate the diffusion of ions. Within 3 h continuous diffusion, the conductivities of all the permeates are consistently in the order of μS cm^{-1} (Figure S30), implying their low concentration. We further find that the salt concentration remarkably affects the permeation behavior of ions (Figure S31), and this should originate from the different concentration gradient. As can be seen from the initial diffusion results, KCl penetrates much slower than NaCl (Figure S32), although K^+ is smaller than Na^+. Besides, the diffusion rates of KCl, NaCl, and Na_2SO_4 in the first 60 min are all relatively lower than that of the following duration, which presents a turning point at the diffusion time of 1 h (Figure 5b, the standard curve of salt solution is given Figure S33). This nonlinear diffusion can be ascribed to the massive adsorption of ions in highly porous sub-nanometer channels, as verified by the static adsorption results (Figure S34).[37] The adsorption of ions in sub-nanometer pores, thus forming a continuous ionic transporting route to deliver ions and water, could promote the diffusion of these small ions.[38] Stable diffusion rates for various ions were then calculated based on the ionic conductivities of the final 2 h. As shown in Figure 5c, the permeation rate of various ions scales inversely with their hydrated diameters, that is, $K^+ > Na^+ > Cu^{2+} > Al^{3+}$. As a result, the 3D COF-1 membrane exhibits a sharp cutoff at ∼8.3 Å, matching well with its effective pore diameter.[30] Significantly, our 3D COF-1 membrane achieves a pronounced K^+/Na^+ selectivity of ∼2.4, which is comparable or higher than that of the metal−organic framework and graphene-based synthetic membranes specially engineered for recovering alkali metal ions.[39−41] The ion selectivities for monovalent/multivalent ions, K^+/Cu^{2+}, K^+/Al^{3+}, Na^+/Cu^{2+}, and Na^+/Al^{3+}, are as high as 84.3, 823.5, 35.3, and 345.3, respectively (Figure 5d). After a decade-long study, membranes with sub-nanometer channels have been developed to separate ions.[42−44] Particularly, the aperture size, structural regularity, and pore wall functions of those membranes are vital for precise ion sieving.[45,46] Here, thanks to the uniform configuration with sub-nanometer pathways, 3D COF-1 membranes are available for efficient ion sieving.

The channel size of 3D COF membranes is molecularly contrivable by adopting suitable monomers to satisfy the requirement for separating fine targets, free of any complicated or tedious modification procedures. As a proof of concept, the 3D COF-4 membrane with intrinsic 14 Å channels[30] was used to fractionate small organic molecules from their mixtures. As can be seen from the UV−vis spectra in Figure 5e, methyl orange (MO) (M_w = 327.3 Da, size = 0.6 nm × 1.1 nm) can freely pass through the 3D COF-4 membrane, while Evans blue (EB) (M_w = 960.8 Da, size = 1.2 nm × 3.1 nm) is largely repelled without noticeable penetration. The appearance change of the permeate from initially colorless to orange further substantiates the exclusive penetration of MO as the dark blue EB is not involved (Figure S35).[12] Thus, synthesizing 3D COF membranes with long linkers provides a facile route to generate nanoscale channels suited for molecular sieving. Significantly, the adjustability of pore sizes ranging from <1 to ∼1.5 nm benefits the design of membranes for both ion sieving and molecular separation (Figure 5f), obviously outperforming the conventional materials.

CONCLUSIONS

In summary, we have demonstrated an oligomer interfacial ripening strategy to produce pore-tailored 3D COF membranes with interpenetrated channels for efficient ionic and molecular sieving. Organized interlacement of building units in the three dimension endows these membranes with narrow and uniform aperture sizes as well as additional mass transfer pathways, thus offering a largely improved separation precision and efficiency. The design concept from the oligomer level strategically provides accurate control over the membrane structure and shows an excellent universality to prepare imine-

https://doi.org/10.1021/acs.macromol.1c02333
Macromolecules 2022, 55, 3259−3266

linked 3D COF membranes. By altering the linker sizes, we thereby obtain several kinds of 3D COF membranes featuring nanochannels with the size in the range of ~0.8−1.5 nm. On account of the synergy between fine aperture pores and interpenetrated structures, the 3D COF membranes demonstrate prominent ion selectivities between monovalent and multivalent ions up to several hundred and a precise fractionation of molecular mixtures. Therefore, this work develops a new avenue toward engineering robust COF membranes and may advance the development and potential application of 3D framework materials.

■ ASSOCIATED CONTENT

Supporting Information

The Supporting Information is available free of charge at https://pubs.acs.org/doi/10.1021/acs.macromol.1c02333.

Experimental procedures; diagrams of the membrane synthesis and ion diffusion; oligomerization of monomers; pore structure determination of 3D COFs; morphologies of 3D COF membranes; dye and ion diffusion results; ion adsorption results; and molecular sieving results (PDF)

Stability demonstration of the 3D COF-1 membrane (MP4)

■ AUTHOR INFORMATION

Corresponding Author

Yong Wang − *State Key Laboratory of Materials-Oriented Chemical Engineering and College of Chemical Engineering, Nanjing Tech University, Nanjing 211816, P. R. China;* orcid.org/0000-0002-8653-514X; Email: yongwang@njtech.edu.cn

Authors

Xiansong Shi − *State Key Laboratory of Materials-Oriented Chemical Engineering and College of Chemical Engineering, Nanjing Tech University, Nanjing 211816, P. R. China;* orcid.org/0000-0002-4258-7941

Zhe Zhang − *State Key Laboratory of Materials-Oriented Chemical Engineering and College of Chemical Engineering, Nanjing Tech University, Nanjing 211816, P. R. China*

Mingjie Wei − *State Key Laboratory of Materials-Oriented Chemical Engineering and College of Chemical Engineering, Nanjing Tech University, Nanjing 211816, P. R. China;* orcid.org/0000-0001-7601-4749

Xingyuan Wang − *State Key Laboratory of Materials-Oriented Chemical Engineering and College of Chemical Engineering, Nanjing Tech University, Nanjing 211816, P. R. China*

Jingtao Wang − *School of Chemical Engineering, Zhengzhou University, Zhengzhou, Henan 450001, P. R. China;* orcid.org/0000-0002-2004-9640

Yatao Zhang − *School of Chemical Engineering, Zhengzhou University, Zhengzhou, Henan 450001, P. R. China;* orcid.org/0000-0002-6832-3127

Complete contact information is available at: https://pubs.acs.org/10.1021/acs.macromol.1c02333

Author Contributions

The manuscript was written through contributions of all authors. All authors have given approval to the final version of the manuscript.

Notes

The authors declare no competing financial interest.

■ ACKNOWLEDGMENTS

This work was financially supported by the National Natural Science Foundation of China (21825803 and 22008110) and the China Postdoctoral Science Foundation (2020 M681568). We also thank the Project of Priority Academic Program Development of Jiangsu Higher Education Institutions (PAPD).

■ REFERENCES

(1) Ding, S.-Y.; Wang, W. Covalent organic frameworks (COFs): from design to applications. *Chem. Soc. Rev.* **2013**, *42*, 548−568.

(2) Kandambeth, S.; Dey, K.; Banerjee, R. Covalent organic frameworks: Chemistry beyond the structure. *J. Am. Chem. Soc.* **2019**, *141*, 1807−1822.

(3) Fan, C. Y.; Wu, H.; Guan, J. Y.; You, X. D.; Yang, C.; Wang, X. Y.; Cao, L.; Shi, B. B.; Peng, Q.; Kong, Y.; Wu, Y. Z.; Khan, N. A.; Jiang, Z. Y. Scalable Fabrication of Crystalline COF Membranes from Amorphous Polymeric Membranes. *Angew. Chem., Int. Ed.* **2021**, *60*, 18051−18058.

(4) Geng, K. Y.; Arumugam, V.; Xu, H. J.; Gao, Y. N.; Jiang, D. L. Covalent Organic Frameworks: Polymer Chemistry and Functional Design. *Prog. Polym. Sci.* **2020**, *108*, No. 101288.

(5) Song, Y.; Sun, Q.; Aguila, B.; Ma, S. Opportunities of Covalent Organic Frameworks for Advanced Applications. *Adv. Sci.* **2019**, *6*, No. 1801410.

(6) Cote, A. P.; Benin, A. I.; Ockwig, N. W.; O'Keeffe, M.; Matzger, A. J.; Yaghi, O. M. Porous, crystalline, covalent organic frameworks. *Science* **2005**, *310*, 1166−1170.

(7) Guan, X.; Chen, F.; Fang, Q.; Qiu, S. Design and applications of three dimensional covalent organic frameworks. *Chem. Soc. Rev.* **2020**, *49*, 1357−1384.

(8) Warkiani, M. E.; Bhagat, A. A. S.; Khoo, B. L.; Han, J.; Lim, C. T.; Gong, H. Q.; Fane, A. G. Isoporous Micro/Nanoengineered Membranes. *ACS Nano* **2013**, *7*, 1882−1904.

(9) Wang, H.; Wang, M.; Liang, X.; Yuan, J.; Yang, H.; Wang, S.; Ren, Y.; Wu, H.; Pan, F.; Jiang, Z. Organic molecular sieve membranes for chemical separations. *Chem. Soc. Rev.* **2021**, *50*, 5468−5516.

(10) Yuan, S.; Li, X.; Zhu, J.; Zhang, G.; Van Puyvelde, P.; Van der Bruggen, B. Covalent organic frameworks for membrane separation. *Chem. Soc. Rev.* **2019**, *48*, 2665−2681.

(11) Dey, K.; Pal, M.; Rout, K. C.; Kunjattu, S. H.; Das, A.; Mukherjee, R.; Kharul, U. K.; Banerjee, R. Selective Molecular Separation by Interfacially Crystallized Covalent Organic Framework Thin Films. *J. Am. Chem. Soc.* **2017**, *139*, 13083−13091.

(12) Shinde, D. B.; Sheng, G.; Li, X.; Ostwal, M.; Emwas, A.-H.; Huang, K.-W.; Lai, Z. Crystalline 2D covalent organic framework membranes for high-flux organic solvent nanofiltration. *J. Am. Chem. Soc.* **2018**, *140*, 14342−14349.

(13) Dey, K.; Kunjattu, S. H.; Chahande, A. M.; Banerjee, R. Nanoparticle Size-Fractionation through Self-Standing Porous Covalent Organic Framework Films. *Angew. Chem., Int. Ed.* **2020**, *59*, 1161−1165.

(14) Fan, H.; Peng, M.; Strauss, I.; Mundstock, A.; Meng, H.; Caro, J. High-Flux Vertically Aligned 2D Covalent Organic Framework Membrane with Enhanced Hydrogen Separation. *J. Am. Chem. Soc.* **2020**, *142*, 6872−6877.

(15) Liu, C.; Jiang, Y.; Nalaparaju, A.; Jiang, J.; Huang, A. Post-synthesis of a covalent organic framework nanofiltration membrane for highly efficient water treatment. *J. Mater. Chem. A* **2019**, *7*, 24205−24210.

(16) Fan, H.; Peng, M.; Strauss, I.; Mundstock, A.; Meng, H.; Caro, J. MOF-in-COF molecular sieving membrane for selective hydrogen separation. *Nat. Commun.* **2021**, *12*, 1−10.

(17) Fan, H.; Mundstock, A.; Feldhoff, A.; Knebel, A.; Gu, J.; Meng, H.; Caro, J. Covalent Organic Framework-Covalent Organic Framework Bilayer Membranes for Highly Selective Gas Separation. *J. Am. Chem. Soc.* **2018**, *140*, 10094−10098.
(18) El-Kaderi, H. M.; Hunt, J. R.; Mendoza-Cortes, J. L.; Cote, A. P.; Taylor, R. E.; O'Keeffe, M.; Yaghi, O. M. Designed synthesis of 3D covalent organic frameworks. *Science* **2007**, *316*, 268−272.
(19) Fan, C. Y.; Geng, H. B.; Wu, H.; Peng, Q.; Wang, X. Y.; Shi, B. B.; Kong, Y.; Yin, Z. Y.; Liu, Y. Q.; Jiang, Z. Y. Three-Dimensional Covalent Organic Framework Membrane for Efficient Proton Conduction. *J. Mater. Chem. A* **2021**, *9*, 17720−17723.
(20) Shi, X. S.; Zhang, Z.; Fang, S. Y.; Wang, J. T.; Zhang, Y. T.; Wang, Y. Flexible and Robust Three-Dimensional Covalent Organic Framework Membranes for Precise Separations under Extreme Conditions. *Nano Lett.* **2021**, *21*, 8355−8362.
(21) Zhang, Y.; Fang, T.; Hou, Q.; Li, Z.; Yan, Y. Water desalination of a new three-dimensional covalent organic framework: a molecular dynamics simulation study. *Phys. Chem. Chem. Phys.* **2020**, *22*, 16978−16984.
(22) Lu, H.; Wang, C.; Chen, J.; Ge, R.; Leng, W.; Dong, B.; Huang, J.; Gao, Y. A novel 3D covalent organic framework membrane grown on a porous alpha-Al_2O_3 substrate under solvothermal conditions. *Chem. Commun.* **2015**, *51*, 15562−15565.
(23) Fu, J.; Das, S.; Xing, G.; Ben, T.; Valtchev, V.; Qiu, S. Fabrication of COF-MOF Composite Membranes and Their Highly Selective Separation of H_2/CO_2. *J. Am. Chem. Soc.* **2016**, *138*, 7673−7680.
(24) Colson, J. W.; Woll, A. R.; Mukherjee, A.; Levendorf, M. P.; Spitler, E. L.; Shields, V. B.; Spencer, M. G.; Park, J.; Dichtel, W. R. Oriented 2D Covalent Organic Framework Thin Films on Single-Layer Graphene. *Science* **2011**, *332*, 228−231.
(25) Hao, Q.; Zhao, C.; Sun, B.; Lu, C.; Liu, J.; Liu, M.; Wan, L.-J.; Wang, D. Confined Synthesis of Two-Dimensional Covalent Organic Framework Thin Films within Superspreading Water Layer. *J. Am. Chem. Soc.* **2018**, *140*, 12152−12158.
(26) Matsumoto, M.; Valentino, L.; Stiehl, G. M.; Balch, H. B.; Corcos, A. R.; Wang, F.; Ralph, D. C.; Marinas, B. J.; Dichtel, W. R. Lewis-Acid-Catalyzed Interfacial Polymerization of Covalent Organic Framework Films. *Chem* **2018**, *4*, 308−317.
(27) Hu, L.; Chen, M.; Fang, X.; Wu, L. Oil-water interfacial self-assembly: a novel strategy for nanofilm and nanodevice fabrication. *Chem. Soc. Rev.* **2012**, *41*, 1350−1362.
(28) Lin, Y.; Skaff, H.; Emrick, T.; Dinsmore, A. D.; Russell, T. P. Nanoparticle assembly and transport at liquid-liquid interfaces. *Science* **2003**, *299*, 226−229.
(29) Duan, H. W.; Wang, D. Y.; Kurth, D. G.; Mohwald, H. Directing self-assembly of nanoparticles at water/oil interfaces. *Angew. Chem., Int. Ed.* **2004**, *43*, 5639−5642.
(30) Guan, X.; Ma, Y.; Li, H.; Yusran, Y.; Xue, M.; Fang, Q.; Yan, Y.; Valtchev, V.; Qiu, S. Fast, Ambient Temperature and Pressure Ionothermal Synthesis of Three-Dimensional Covalent Organic Frameworks. *J. Am. Chem. Soc.* **2018**, *140*, 4494−4498.
(31) Fischbach, D. M.; Rhoades, G.; Espy, C.; Goldberg, F.; Smith, B. J. Controlling the crystalline structure of imine-linked 3D covalent organic frameworks. *Chem. Commun.* **2019**, *55*, 3594−3597.
(32) Khayum, M. A.; Kandambeth, S.; Mitra, S.; Nair, S. B.; Das, A.; Nagane, S. S.; Mukherjee, R.; Banerjee, R. Chemically delaminated free-standing ultrathin covalent organic nanosheets. *Angew. Chem., Int. Ed.* **2016**, *55*, 15604−15608.
(33) Fan, H.; Gu, J.; Meng, H.; Knebel, A.; Caro, J. High-Flux Membranes Based on the Covalent Organic Framework COF-LZU1 for Selective Dye Separation by Nanofiltration. *Angew. Chem., Int. Ed.* **2018**, *57*, 4083−4087.
(34) Kandambeth, S.; Venkatesh, V.; Shinde, D. B.; Kumari, S.; Halder, A.; Verma, S.; Banerjee, R. Self-templated chemically stable hollow spherical covalent organic framework. *Nat. Commun.* **2015**, *6*, 6786.
(35) Jin, Y.; Hu, Y.; Ortiz, M.; Huang, S.; Ge, Y.; Zhang, W. Confined growth of ordered organic frameworks at an interface. *Chem. Soc. Rev.* **2020**, *49*, 4637−4666.
(36) Jian, M.; Qiu, R.; Xia, Y.; Lu, J.; Chen, Y.; Gu, Q.; Liu, R.; Hu, C.; Qu, J.; Wang, H.; Zhang, X. Ultrathin water-stable metal-organic framework membranes for ion separation. *Sci. Adv.* **2020**, *6*, No. eaay3998.
(37) Ou, R.; Zhang, H.; Truong, V. X.; Zhang, L.; Hegab, H. M.; Han, L.; Hou, J.; Zhang, X.; Deletic, A.; Jiang, L.; Simon, G. P.; Wang, H. A sunlight-responsive metal-organic framework system for sustainable water desalination. *Nat. Sustain.* **2020**, *3*, 1052−1058.
(38) Xu, F.; Wei, M.; Zhang, X.; Wang, Y. Ion Rejection in Covalent Organic Frameworks: Revealing the Overlooked Effect of In-Pore Transport. *ACS Appl. Mater. Interfaces* **2019**, *11*, 45246−45255.
(39) Zhang, H.; Hou, J.; Hu, Y.; Wang, P.; Ou, R.; Jiang, L.; Liu, J. Z.; Freeman, B. D.; Hill, A. J.; Wang, H. Ultrafast selective transport of alkali metal ions in metal organic frameworks with subnanometer pores. *Sci. Adv.* **2018**, *4*, No. aaq0066.
(40) Li, Z.; Zhang, X.; Tan, H.; Qi, W.; Wang, L.; Ali, M. C.; Zhang, H.; Chen, J.; Hu, P.; Fan, C.; Qiu, H. Combustion Fabrication of Nanoporous Graphene for Ionic Separation Membranes. *Adv. Funct. Mater.* **2018**, *28*, No. 1805026.
(41) Ren, C. E.; Hatzell, K. B.; Alhabeb, M.; Ling, Z.; Mahmoud, K. A.; Gogotsi, Y. Charge- and Size-Selective Ion Sieving Through $Ti_3C_2T_x$ MXene Membranes. *J. Phys. Chem. Lett.* **2015**, *6*, 4026−4031.
(42) Sapkota, B.; Liang, W.; VahidMohammadi, A.; Karnik, R.; Noy, A.; Wanunu, M. High permeability sub-nanometre sieve composite MoS_2 membranes. *Nat. Commun.* **2020**, *11*, 2747.
(43) Ding, L.; Li, L.; Liu, Y.; Wu, Y.; Lu, Z.; Deng, J.; Wei, Y.; Caro, J.; Wang, H. Effective ion sieving with $Ti_3C_2T_x$ MXene membranes for production of drinking water from seawater. *Nat. Sustain.* **2020**, *3*, 296−302.
(44) Liu, X.; Demir, N. K.; Wu, Z.; Li, K. Highly Water-Stable Zirconium Metal Organic Framework UiO-66 Membranes Supported on Alumina Hollow Fibers for Desalination. *J. Am. Chem. Soc.* **2015**, *137*, 6999−7002.
(45) Lu, J.; Zhang, H.; Hou, J.; Li, X.; Hu, X.; Hu, Y.; Easton, C. D.; Li, Q.; Sun, C.; Thornton, A. W.; Hill, M. R.; Zhang, X.; Jiang, G.; Liu, J. Z.; Hill, A. J.; Freeman, B. D.; Jiang, L.; Wang, H. Efficient metal ion sieving in rectifying subnanochannels enabled by metal-organic frameworks. *Nat. Mater.* **2020**, *19*, 767−774.
(46) Abraham, J.; Vasu, K. S.; Williams, C. D.; Gopinadhan, K.; Su, Y.; Cherian, C. T.; Dix, J.; Prestat, E.; Haigh, S. J.; Grigorieva, I. V.; Carbone, P.; Geim, A. K.; Nair, R. R. Tunable sieving of ions using graphene oxide membranes. *Nat. Nanotechnol.* **2017**, *12*, 546−550.

https://doi.org/10.1021/acs.macromol.1c02333
Macromolecules 2022, 55, 3259−3266